Microbiology (2012), **158**, 2144–2157 **DOI** 10.1099/mic.0.058404-0

Outer-membrane cytochrome-independent reduction of extracellular electron acceptors in *Shewanella oneidensis*

Clemens Bücking,[1] Annette Piepenbrock,[2] Andreas Kappler[2] and Johannes Gescher[1]

Correspondence
Johannes Gescher
johannes.gescher@kit.edu

[1]Institut für angewandte Biowissenschaften, Angewandte Biologie, Karlsruher Institut für Technologie, Fritz-Haber-Weg 2, D-76131 Karlsruhe, Germany

[2]Geomicrobiology, Center for Applied Geosciences, University of Tübingen, Sigwartstrasse 10, D-72076 Tübingen, Germany

Dissimilatory metal reduction under pH-neutral conditions is dependent on an extended respiratory chain to the cell surface. The final reduction is catalysed by outer-membrane cytochromes that transfer respiratory electrons either directly to mineral surfaces and metal ions bound in larger organic complexes such as Fe(III) citrate, or indirectly using endogenous or exogenous electron shuttles such as humic acids and flavins. Consequently, a *Shewanella oneidensis* deletion mutant devoid of outer-membrane cytochromes is unable to reduce Fe(III) citrate or manganese oxide minerals and reduces humic acids at lower rates. Surprisingly, the phenotype of this quintuple deletion mutant can be rescued by a suppressor mutation, which enables metal or humic acid reduction without any outer-membrane cytochrome. Furthermore, the type II secretion system, essential for metal reduction in wild-type *S. oneidensis*, is not necessary for the suppressor strain. Using genome sequencing we identified two point mutations in key genes for metal reduction: *mtrA* and *mtrB*. These mutations are necessary and sufficient to account for the observed phenotype. This study is the first evidence for a catabolic, outer-membrane cytochrome-independent electron transport chain to ferric iron, manganese oxides and humic acid analogues operating in a mesophilic organism. Available bioinformatic data allow the hypothesis that outer-membrane cytochrome-independent electron transfer might resemble an evolutionary intermediate between ferrous iron-oxidizing and ferric iron-reducing micro-organisms.

Received 8 February 2012
Revised 31 March 2012
Accepted 2 April 2012

INTRODUCTION

Bacterial dissimilatory metal reduction has been investigated intensely in the last few decades. This is due to its relevance as a respiratory process in a multitude of environments, and the possible applications in biotechnology such as remediation of contaminated soils and electricity production in microbial fuel cells. One of the best-studied model organisms is *Shewanella oneidensis* MR-1, a γ-proteobacterium with 41 putative *c*-type cytochromes encoded in its genome (Meyer *et al.*, 2004; Romine *et al.*, 2008).

Several of these *c*-type cytochromes have been shown to form a respiratory network extending the respiratory chain from the cytoplasmic membrane through the periplasm to the outer membrane (Schuetz *et al.*, 2009; Shi *et al.*, 2007). From there, catabolic electrons are transferred directly or indirectly to a wide variety of terminal electron acceptors that are either poorly soluble or soluble but unable to pass the outer membrane. Examples of poorly soluble electron acceptors are iron(III) (oxyhydr)oxides such as haematite and ferrihydrite, and manganese oxides such as birnessite and pyrolusite. These minerals are ubiquitously distributed in soils and sediments. Examples of substances that are soluble but apparently unable to pass the outer membrane at least to an extent that supports growth are Fe(III) citrate and the humic acid analogue anthraquinone-2,6-disulfonate (Dobbin *et al.*, 1996; Gescher *et al.*, 2008; Pitts *et al.*, 2003; Shyu *et al.*, 2002).

In *S. oneidensis*, the reduction of most extracellular electron acceptors is based on a protein complex formed by MtrA, MtrB and MtrC (mtr: metal reducing). This complex is most probably the extracellular terminal reductase (Hartshorne *et al.*, 2009; Shi *et al.*, 2006). The current model is that the decahaem *c*-type cytochromes MtrA, localized to the periplasmic side, and MtrC, localized to the outer surface of

Abbreviations: AQDS, anthraquinone-2,6-disulfonate; NTA, nitrilotriacetic acid; PPHA, Pahokee peat humic acids.

Five supplementary figures and two supplementary tables are available with the online version of this paper.

the outer membrane, are held in close proximity via the outer membrane-spanning β-barrel protein MtrB. This close proximity is thought to enable electron transfer through the outer membrane (Hartshorne *et al.*, 2009). OmcA (outer membrane cytochrome), another decahaem *c*-type cytochrome, is also localized to the cell surface and apparently involved in the reduction of manganese oxides (Bücking *et al.*, 2010; Myers & Myers, 2003). Although *in vitro* evidence has been provided for a high-affinity complex between OmcA and MtrC, it seems that they are not colocalized *in vivo* (Lower *et al.*, 2009; Shi *et al.*, 2006; Zhang *et al.*, 2008). Both proteins are lipoproteins that are exported through the outer membrane by the type II secretion system (Shi *et al.*, 2008).

Different models have been proposed of how the terminal metallic electron acceptor is finally reduced. MtrC and OmcA have been shown to directly reduce iron minerals *in vitro* (Reardon *et al.*, 2010; Xiong *et al.*, 2006). The transfer rates to ferric iron are rather low and cannot explain entirely the fast rates of iron reduction by whole cells. It has therefore been proposed that endogenous flavin redox shuttles are involved in this electron transfer process (Marsili *et al.*, 2008; Ross *et al.*, 2009; von Canstein *et al.*, 2008). However, reduction of the flavin shuttle molecules depends on the whole electron transfer chain, since they apparently cannot pass the outer membrane and therefore also have to be reduced by outer-membrane cytochromes (Coursolle *et al.*, 2010; Richter *et al.*, 2010). In the aquatic sediments from which *S. oneidensis* MR-1 was originally isolated, humic acids are frequently present (Myers & Nealson, 1988a; Stevenson, 1994). They represent exogenous electron shuttles. Consequently, it was shown that Fe(III) reduction by *S. oneidensis* was stimulated by humic substances at concentrations as low as 5–10 mg carbon l^{-1}. Humic substances can occur in dissolved or solid-phase form. Both have been studied extensively with respect to their effect on microbial Fe(III) reduction due to electron shuttling (Jiang & Kappler, 2008; Lovley *et al.*, 1996; Roden *et al.*, 2010).

Another possible mode of electron transfer is represented by so-called nanowires, which were first described by Reguera and co-workers for *Geobacter sulfurreducens* and shortly afterwards by Gorby and co-workers for *S. oneidensis* (Gorby *et al.*, 2006; Reguera *et al.*, 2005). It was hypothesized that these cell appendages can transfer electrons to an electron acceptor that is not in direct contact with the cell but rather located distantly from it. In *S. oneidensis*, electron transfer along the pilus is dependent on the presence of MtrC and OmcA (El-Naggar *et al.*, 2010). Probably, all three modes of electron transfer (i.e. direct contact, electron shuttling and nanowires) operate simultaneously, but all of them fundamentally rely on the catalytic activity of outer-membrane *c*-type cytochromes.

In this study we report that a quintuple deletion mutant devoid of genes for outer-membrane cytochromes (Bücking *et al.*, 2010) can regain the ability to reduce extracellular electron acceptors such as ferric iron, manganese dioxide, humic acids and anthraquinone-2,6-disulfonate (AQDS), a model compound for quinone moieties in humic acids. This mutant is not affected in outer-membrane stability, which excludes an increased reduction of extracellular electron acceptors by periplasmic *c*-type cytochromes. Resequencing of the mutant genome and subsequent mapping to the *S. oneidensis* reference genome revealed that one point mutation in MtrA and one in MtrB are the reasons for the evolution of an extended respiratory chain independent of outer-membrane cytochromes.

METHODS

Reagents. Chemicals and biochemicals were obtained from Sigma-Aldrich, Roth and Promega. Enzymes were purchased from New England Biolabs.

Growth conditions and media. All micro-organisms used in this study are listed in Table 1. *Escherichia coli* strains were grown aerobically in Luria–Bertani (LB) medium at 37 °C. *Saccharomyces cerevisiae* InvSc1 was grown on YPD medium and was selected for transformants on uracil-free medium purchased from Clontech. *S. oneidensis* strains were grown aerobically at 30 °C in LB medium or in minimal medium under anoxic conditions, supplemented with lactate (50 mM) as electron donor and carbon source, and 50 mM Fe(III) citrate, 5 mM Fe(III) nitrilotriacetic acid (NTA) or 100 mM fumarate as electron acceptor, as described previously (Schuetz *et al.*, 2009). Fe(III) citrate powder was dissolved in hot water and pH was adjusted to pH 7.4 slowly with 1 M NaOH. If necessary, kanamycin (50 μg ml^{-1}), arabinose (1 mM) or 2,6-diaminopimelic acid (100 μg ml^{-1}) was added to the medium. Fe(III) citrate and NTA-complexed ferric iron [Fe(III)-NTA] reduction was determined by measuring ferrous iron concentrations with the ferrozine reagent (Stookey, 1970), and was used as a surrogate for bacterial growth. For growth experiments with birnessite (manganese dioxide) as electron acceptor, 2.5 mM birnessite was added to minimal medium that was supplemented with 1 mM arabinose. Birnessite was prepared as described earlier (Burdige & Nealson, 1985). Manganese reduction was determined in three independent cultures using leucoberbellin blue (Boogerd & de Vrind, 1987). The rate of abiotic Mn(IV) decrease in culture flasks was subtracted from the measured values.

Standard procedures. Membrane fractions were prepared as described previously (Schuetz *et al.*, 2009). Protein concentrations were determined by the method of Bradford (1976) with BSA as standard. Proteins were separated on polyacrylamide gels according to Laemmli (1970). Haem proteins were visualized by peroxidase staining (Thomas *et al.*, 1976). Proteins containing a C-terminal strep-tag were detected on a Western blot using a strep-tag antibody (Qiagen).

Construction of markerless *S. oneidensis* mutants. Strains containing Δ*gspD*, Δ*dmsA-1 dmsB-1* and Δ*dmsA-2 dmsB-2* deletions were constructed according to Schuetz *et al.* (2009), with minor modifications. All primers used are listed in Table S1. Primers 1–4 were used to amplify 500 bp regions up- and downstream of *gspD*. The resulting fragments were cloned into a linearized pMQ150 plasmid using a *Saccharomyces cerevisiae*-based recombination system (Shanks *et al.*, 2006). The resulting plasmid pMQ150-Δ*gspD* was transformed into *E. coli* WM3064, which was then used as donor strain for conjugation-based mating with *S. oneidensis*. Primers 5–8 were used to construct pMQ150-Δ*dmsA-1 dmsB-1*, and primers 9–12 were used to assemble pMQ150-Δ*dmsA-2 dmsB-2*.

Genome sequencing. Genomic DNA was isolated using the Illustra bacteria genomicPrep kit (GE Healthcare) according to the manufacturer's

Table 1. Yeast and bacterial strains used in this study

Strain no.	Strain	Relevant genotype	Reference or source
JG98	*E. coli* WM3064	*thrB1004 pro thirpsLhsdS lacZ*ΔM15 *RP4–1360* Δ(*araBAD*)*567* Δ*dapA1341*::[*ermpir*(*wt*)]	Saltikov & Newman (2003)
JG22	*E. coli* DH5α Z1	*aci*^{q}, *PN25-tetR*, *Sp*^{R}, *deoR*, *supE44*, Δ(*lacZYA-argFV169*), ϕ80 *lacZ* ΔM15	Lutz & Bujard (1997)
JG26	*Saccharomyces cerevisiae* InvSc1	*MATa/MATα leu2/leu2 trp1-289/trp1-289 ura3-52/ura3-52 his3-Δ1/his3-Δ1*	Invitrogen
JG7	*S. oneidensis* MR-1	Wild-type	Venkateswaran *et al.* (1999)
JG132	*S. oneidensis* MR-1 ΔOMC (outer-membrane cytochrome deletion mutant)	Δ(*mtrD-mtrC*) ΔSO_2931 ΔSO_1659, 3100633::(araC, P_{BAD})	Bücking *et al.* (2010)
JG12	*S. oneidensis* MR-1 ΔOMC^{S} (suppressor of outer-membrane cytochrome deletion mutant)	ΔOMC *mtrA*: position 869 C to A, *mtrB*: position 656 C to A	This study
JG202	*E. coli* WM3064 pMQ150ΔgspD	pMQ150ΔdgspD	This study
JG411	*E. coli* WM3064 pMQ150ΔdmsA-1 dmsB-1	pMQ150ΔdmsA-1 dmsB-1	This study
JG305	*E. coli* WM3064 pMQ150ΔdmsA-2 dmsB-2	pMQ150ΔdmsA-2 dmsB-2	This study
JG450	*S. oneidensis* MR-1 ΔOMC pmtrA mtrB	pmtrAmtrB	This study
JG462	*S. oneidensis* MR-1 ΔOMC pmtrA^{S}	pmtrA^{S}	This study
JG463	*S. oneidensis* MR-1 ΔOMC pmtrB^{S}	pmtrB^{S}	This study
JG449	*S. oneidensis* MR-1 ΔOMC pmtrA^{S}mtrB^{S}	pmtrA^{S}mtrB^{S}	This study
JG434	*S. oneidensis* MR-1 ΔOMC^{S} Δ*dmsA-1* Δ*dmsB-1* Δ*dmsA-2* Δ*dmsB-2*	ΔOMC^{S} Δ*dmsA-1* Δ*dmsB-1* Δ*dmsA-2* Δ*dmsB-2*	This study
JG444	*S. oneidensis* MR-1 ΔOMC^{S}Δ*gspD*	ΔOMC^{S}Δ*gspD*	This study
JG443	*S. oneidensis* MR-1	Δ*gspD*	This study
JG52	*S. oneidensis* MR-1 Δ*mtrA*	Δ*mtrA*	Schuetz *et al.* (2009)
JG55	*S. oneidensis* MR-1 Δ*mtrB*	Δ*mtrB*	Schuetz *et al.* (2009)
JG468	*S. oneidensis* MR-1 Δ*mtrA* pmtrA^{S}	Δ*mtrA* pmtrA^{S}	This study
JG469	*S. oneidensis* MR-1 Δ*mtrB* pmtrB^{S}	Δ*mtrB* pmtrB^{S}	This study
JG474	*S. oneidensis* MR-1 ΔOMC^{S} pmtrAmtrB^{S}	ΔOMC^{S} pmtrAmtrB^{S}	This study

instructions. Sequencing was performed on an Illumina HiSeq 2000 with a read length of 46 bp by GATC Biotech. The reads were assembled using the software BWA (Li & Durbin, 2009), and identification of single nucleotide polymorphisms as well as insertions and deletions was done with SAMtools (Li *et al.*, 2009) and the assembly viewer Tablet (Milne *et al.*, 2010).

Cloning of *mtrA* and *mtrB* and their mutated versions. Genomic DNA of either *S. oneidensis* wild-type or ΔOMC^{S} was used as a template to amplify *mtrA* (primers 13, 14), *mtrB* (primers 15, 16) or *mtrA* and *mtrB* (primers 13, 16). Primer 16 contains furthermore the sequence for a strep-tag, which was added to the C terminus of MtrB. The target vector pBAD202 was digested with *Nco*I and *Pme*I. Vector and inserts were purified and then assembled via isothermal DNA assembly (Gibson *et al.*, 2009). The overlap between PCR fragment and linearized plasmid was 50 bp long. To construct a plasmid with a combination of wild-type *mtrA* and mutated *mtrB*, we amplified an *mtrA*-fragment with primers 13 and 17 and an *mtrB*^{S} fragment, containing the point mutation, with primers 18 and 16. Both fragments were combined in one step with the same method as above. All resulting plasmids were sequenced (GATC Biotech).

Ferric iron reduction cell suspension assays. Cells were grown under anoxic conditions overnight in minimal medium with fumarate as electron acceptor, and with 1 mM arabinose to induce *mtrA* and *mtrB* expression (*mtrA* and *mtrB* are under arabinose promoter control in ΔOMC cells) (Bücking *et al.*, 2010). Cells were harvested and washed twice using minimal medium without fumarate and lactate under anoxic conditions, and resuspended to a final OD_{600} between 3 and 5. Specific reduction rates of independent triplicate cultures were obtained by normalization to the protein content of the cell suspension. Fifty microlitres of cell suspension was pipetted into a well of a microtitre plate. The assay was started by the addition of 150 µl of a solution containing 10 mM lactate and 10 mM Fe(III) citrate. At different time points (0–30 min) the reaction was stopped by the addition of 100 µl 3 M HCl. The Fe^{2+} concentration of the samples was determined using the ferrozine reagent (Stookey, 1970).

Riboflavin and AQDS reduction rates. Cells for these assays were grown under anoxic conditions with fumarate as electron acceptor and, if necessary, in the presence of arabinose as inductor for gene expression. Cells were harvested and washed twice before the start of the experiments. Riboflavin reduction was measured in cuvettes with butyl rubber stoppers at 30 °C and 450 nm. The assay contained 60 µM riboflavin, 100 mM HEPES, pH 7.4 and 10 mM lactate, and was initiated by the addition of riboflavin. Reduction rates were calculated as a function of protein concentration in the assay. AQDS reduction was measured in a similar assay at a wavelength of 436 nm using 1 mM AQDS (molar absorption coefficient 3500 M^{-1} cm^{-1}; Bayer *et al.*, 1996). Both assays were typically finished within 20 min.

Humic acid reduction rates. Humic acid reduction was measured continuously over 18 days. Pahokee peat humic acids (PPHA), purchased from the International Humic Substances Society (IHSS), were added at a concentration of 1 g l^{-1} with 2 mM lactate as electron donor. At selected time points, samples were withdrawn and the oxidation state of humic acids was analysed by an electron shuttling assay similar to that described earlier (Lovley *et al.*, 1996). Briefly, under anoxic conditions, samples were filtered (0.2 µm) and reacted with 5 mM Fe(III) citrate for 1 h. Subsequently, the sample/Fe(III) citrate mixture was diluted 1 : 2 with 1 M HCl, humic acids were precipitated and removed by centrifugation, and the Fe(II)

concentration was determined by the ferrozine assay (Stookey, 1970). The reducing capacity in micro electron equivalents (μeq l^{-1}) was calculated as the amount of electrons transferred to Fe(III), i.e. the amount of Fe(II) formed. The amount of electrons transferred by the bacteria to humic acids was calculated by subtracting the abiotic reducing capacity of the sterile control from the reducing capacity of the humic acids at the respective time points. Experiments were performed in independent duplicates.

Outer-membrane integrity testing. For outer-membrane integrity testing, cells were grown under anoxic conditions with fumarate as electron acceptor and in the presence of 1 mM arabinose. After washing the cells twice with 100 mM HEPES, pH 7.4, first an ethidium bromide influx assay was performed to measure outer-membrane permeability. The assay was performed according to Murata *et al.* (2007) with minor modifications. The assay was initiated by the addition of ethidium bromide (final concentration 6 μM). Fluorescence was measured continuously over 5 min (excitation and emission wavelengths of 545 and 600 nm, respectively) using a microtitre plate reader (Varioscan, ThermoFisher). Ethidium bromide influx rates are displayed as relative fluorescence units (RFU) per minute and milligram protein. As a positive control, 1 mg polymyxin B ml^{-1} was added to the cells. Polymyxin B destabilizes the membrane and increases permeability (Vaara, 1992).

Second, iron diffusion into the cells was measured after 30 min incubation with 10 mM Fe(III) citrate but without the electron donor at room temperature. Afterwards, the cells were washed twice and acidified to a final concentration of 1 M HCl. All Fe(III) was reduced with 2.5 % (w/v) hydroxylamine hydrochloride and the total iron content was determined with the ferrozine assay (Stookey, 1970). As a positive control, polymyxin B was added at a concentration of 50 μg ml^{-1}. A lower polymyxin B concentration was chosen because of the longer incubation time of this experiment. The iron content was calculated as a function of protein content.

As a third test, antibiotic susceptibility was tested in a disc diffusion test. One hundred microlitres of cell suspension (OD_{600} 0.132, corresponding to McFarland standard 0.5) was spread on LB plates supplemented with 1 mM arabinose, and subsequently paper discs containing 25 μg colistin, 30 μg kanamycin or 30 μg chloramphenicol (Oxoid, Thermo Fisher) were applied to the surface. After overnight incubation at 30 °C, plates were photographed and zones of inhibition were measured with ImageJ (http://imagej.nih.gov/ij/).

Bioinformatic analysis. The integrated microbial genomes tool of the Joint Genome Institute was used to search in available microbial genomes for homologues of *mtrAB* gene cassettes (http://img.jgi.doe.gov). The analysis was performed using the BLASTP algorithm and a concatamer of the protein sequences of MtrA and MtrB from *S. oneidensis*. Detected *mtrAB*-like gene clusters were analysed for genes encoded upstream and downstream of *mtrA*. Only gene clusters that did contain *mtrAB* gene clusters without genes homologous to *mtrC* or *mtrF* were further analysed.

RESULTS

Evolution of a ΔOMC suppressor mutant

Previously we deleted in *S. oneidensis* all five genes that encode outer-membrane cytochromes. Additionally, a P_{BAD} promoter was inserted in the genome of this strain upstream of *mtrA* and *mtrB*, two genes essential for metal reduction. The deletion of the outer-membrane cytochromes resulted in an almost complete loss of the ability to reduce poorly soluble electron acceptors (Bücking *et al.*, 2010). In Fe(III) citrate medium, the Fe(II) concentration did not climb above 2.5 mM within 35 h, and a reduction rate for the ΔOMC strain could thus not be calculated (Fig. 1). However, this minimal Fe(III) citrate-reducing activity apparently increased substantially during prolonged incubation and several serial transfers. The accelerated iron reduction over time suggested the development of a suppressor mutation. In order to characterize a potential suppressor mutant, ΔOMC^S, single cells were isolated using dilution series and subsequent plating on LB agar plates.

Fe(III) citrate, Fe(III)-NTA and birnessite reduction without outer-membrane cytochromes

It has been shown that *S. oneidensis* can couple growth to the reduction of ferric iron or manganese oxides (Myers & Nealson, 1988a, b). Therefore, ferrous iron concentrations were determined as a surrogate for growth in medium containing lactate as carbon and electron source and 50 mM Fe(III) citrate or 5 mM Fe(III)-NTA as electron acceptor. Iron reduction curves were recorded in the presence and absence of 1 mM arabinose as inducer for *mtrA* and *mtrB* expression (Fig. 1). Induction with 1 mM arabinose led to the expression of wild-type levels of MtrA, as determined by SDS-PAGE and staining of haem-containing proteins (Fig. S1). Of note, *S. oneidensis* cannot grow with arabinose as a substrate (Gralnick *et al.*, 2006). As indicated in Fig. 1, Fe(III) citrate reduction of the suppressor mutant ΔOMC^S was strictly dependent on arabinose induction, upon which the reduction rate reached 84 % of the

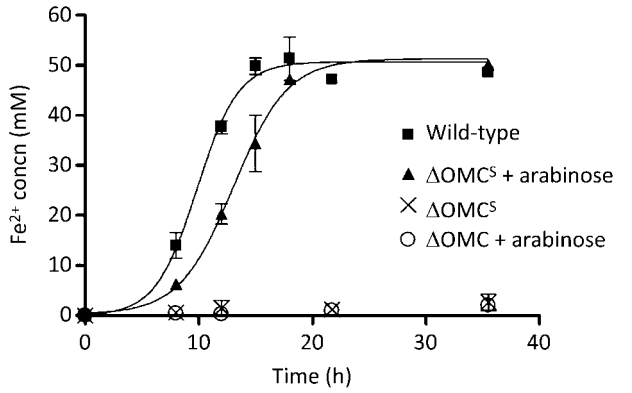

Fig. 1. Fe(III) citrate reduction. Iron reduction by *S. oneidensis* strains growing on minimal medium with 50 mM lactate and 50 mM Fe(III) citrate, and addition of 1 mM arabinose, where indicated. Symbols show means of triplicate measurements; error bars, SD. Solid lines represent curve-fits done with GraphPad Prism 4. The specific iron reduction rate, μ, in h^{-1} was calculated for each biological replicate, and the mean ± SD values are: wild-type, 0.534 ± 0.045; ΔOMC^S + arabinose, 0.451 ± 0.104; reduction rates not determinable for ΔOMC^S and ΔOMC + arabinose because curve-fits were not possible due to minimal reduction within the time frame of the experiment.

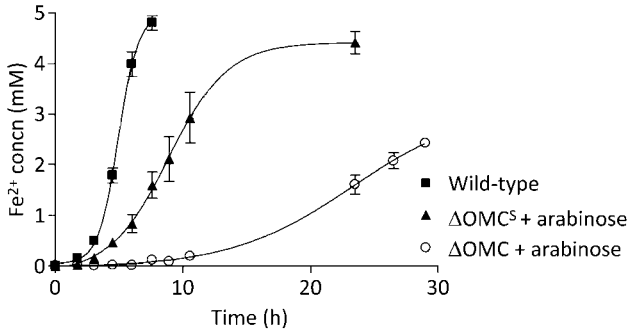

Fig. 2. Fe(III)-NTA reduction. Iron reduction by *S. oneidensis* strains growing on minimal medium with 10 mM lactate and 5 mM Fe(III)-NTA and addition of 1 mM arabinose. Symbols show means of triplicate measurements; error bars, SD. Solid lines represent curve-fits done with GraphPad Prism 4. The specific iron reduction rate, μ, in h^{-1} was calculated for each biological replicate, and the mean ± SD values are: wild-type, 1.3 ± 0.165; ΔOMC^S + arabinose, 0.438 ± 0.081; ΔOMC + arabinose 0.209 ± 0.03.

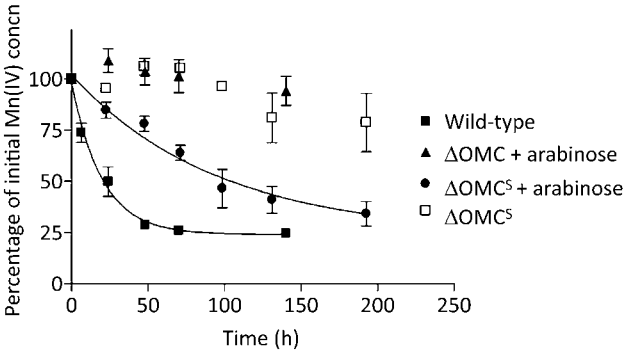

Fig. 3. Birnessite reduction. Manganese reduction was quantified in growth experiments. Birnessite (2.5 mM) was added to 50 ml mineral medium with lactate as an electron donor and 1 mM arabinose, where indicated. The percentage Mn(IV) concentration is relative to the starting concentration. Initial values for Mn(IV) concentration varied slightly (± 0.266 mM) and were therefore set to 100 %. The abiotic decrease in the measurable Mn(IV) concentration (probably due to adhesion to the culture flask) was subtracted. Symbols show means of triplicate measurements; error bars, SD. Solid lines represent curve-fits done with GraphPad Prism 4. The specific Mn(IV) reduction rate, μ, in h^{-1} was calculated for each biological replicate, and the mean ± SD values are: wild-type, 0.051 ± 0.008; ΔOMC^S, 0.008 ± 0.002; reduction rates were not determinable for ΔOMC^S + arabinose and ΔOMC + arabinose because curve-fits were not possible due to minimal reduction within the time frame of the experiment.

wild-type rate (Fig. 1), while the original mutant ΔOMC showed almost no Fe(III) citrate reduction activity. Fe(III)-NTA, which is a smaller and more membrane-permeable iron chelate, was reduced rather slowly by ΔOMC but much faster by the suppressor mutant ΔOMC^S, reaching 34 % of the wild-type reduction rate (Fig. 2).

Birnessite, as a mineral-phase electron acceptor, was used to assess the ability of ΔOMC^S to reduce oxidized manganese species (Fig. 3). While ΔOMC had only background reducing activity, ΔOMC^S was able to reduce birnessite 10-fold faster compared with the original mutant and with 20 % of the wild-type rate. However, the phenotype of birnessite reduction of ΔOMC^S was not as pronounced as with Fe(III) citrate as electron acceptor.

Reduction of electron shuttles by ΔOMC^S

Electron shuttles have been proposed to be involved in *S. oneidensis*-catalysed metal and mineral reduction. Either they can be produced and secreted by the cell endogenously, mainly in the form of riboflavin (Marsili *et al.*, 2008; von Canstein *et al.*, 2008), or they can be present in soils, typically in the form of dissolved or solid-phase humic substances (Jiang & Kappler, 2008; Roden *et al.*, 2010). As humic substances are a structurally diverse group of substances, AQDS can be used as a surrogate for small fulvic acid molecules and for quinone moieties in humic acids (Jiang & Kappler, 2008). Reduction of large humic acid molecules was measured with PPHA.

For riboflavin and AQDS, the reduction activity was recorded over 20 min using washed cell suspensions of anoxically grown cells that should be free of any additional electron shuttle. As Fig. 4(a) indicates, reduction of riboflavin was rather slow for ΔOMC and ΔOMC^S (12 and 21 % of wild-type activity, respectively). In contrast to this, AQDS was reduced by the suppressor mutant with 81 % of the wild-type rate, while the original ΔOMC strain reduced AQDS with only 32 % of the wild-type rate (Fig. 4b). This effect was even more pronounced when the cells were pregrown on Fe(III) citrate, leading to a ΔOMC^S AQDS reducing activity of 99 % compared with the wild-type (Fig. 4b).

The reduction of PPHA was measured over a time frame of 18 days in a growth experiment (Fig. 5). For the reduction of PPHA, the situation resembled the results of the riboflavin reduction experiments. The maximal PPHA reduction rate reached in ΔOMC was 18 % and in ΔOMC^S 35 % of wild-type activity (Fig. 5).

Reduction of Fe(III) citrate by washed cell suspensions

Cell suspension experiments were conducted to assess the ability of ΔOMC^S cells to reduce Fe(III) citrate without the putative involvement of endogenous electron shuttles. The different *S. oneidensis* strains were pre-grown on minimal medium with fumarate or Fe(III) citrate as electron acceptors. Cells were then washed twice in buffer without electron acceptor under anoxic conditions and thereafter used for Fe(III) citrate reduction assays. Fumarate-grown ΔOMC^S cells reduced Fe(III) citrate with 28 % of the wild-type rate, while ΔOMC showed no detectable activity. When the cells

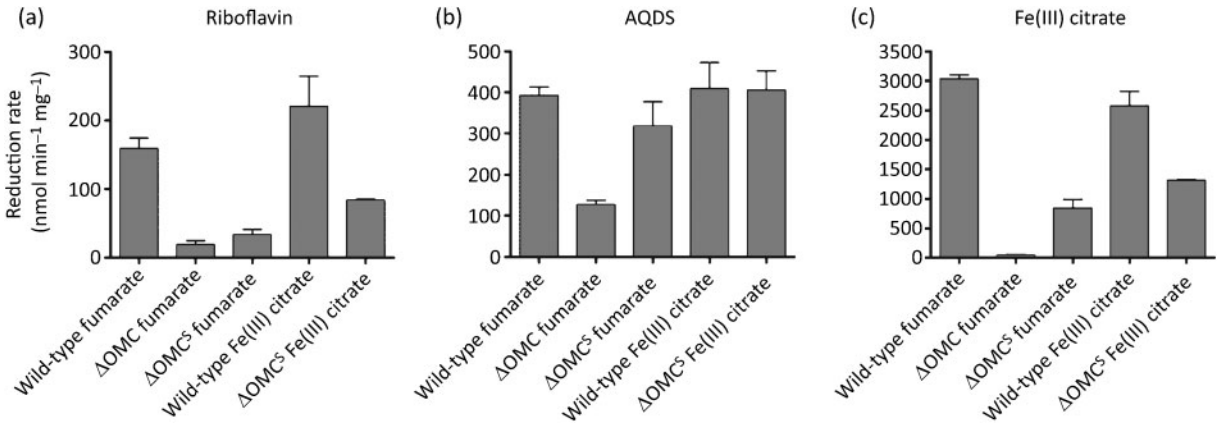

Fig. 4. Cell suspension experiments. Reduction rates of *S. oneidensis* wild-type, ΔOMC mutant and ΔOMC^S mutant strains with riboflavin, AQDS and Fe(III) citrate. Washed cell suspensions were prepared from cultures grown under anoxic conditions with fumarate or Fe(III) citrate as terminal electron acceptor. All experiments were carried out under anoxic conditions. Maximal reduction rates (means of triplicate measurements) were normalized to the protein content. The reduction of riboflavin (a) and AQDS (b) was measured in a continuous spectrophotometric assay using absorption maxima at 450 and 436 nm, respectively. Fe(III) citrate reduction rates (c) were measured by determining Fe(II) content discontinuously using the ferrozine reagent.

were pre-grown on Fe(III) citrate, the activity of ΔOMC^S increased to 51 % of the wild-type ferric iron reduction rate (Fig. 4c).

Putative involvement of other outer-membrane protein complexes

Several experimental results point towards the role of the outer-membrane *c*-type cytochromes MtrC and OmcA as the final metal and flavin reductases of *S. oneidensis* (Bücking *et al.*, 2010; Coursolle *et al.*, 2010). The mechanism of metal reduction in ΔOMC^S must be independent of these proteins and any other outer-membrane cytochrome encoded in the genome of the strain, since all five corresponding genes were deleted (Bücking *et al.*, 2010). A recent study described the modularity of different outer membrane-spanning complexes in *S. oneidensis* (Coursolle & Gralnick, 2010). Hence, it was asked whether another surface-localized terminal reductase could functionally replace outer-membrane cytochromes. The only other enzyme fulfilling this prerequisite is the DMSO reductase DmsAB (Gralnick *et al.*, 2006). The genome of *S. oneidensis* has two gene clusters encoding DMSO reductases (*dmsA-1* and *dmsB-1*, SO_1429–30 and *dmsA-2* and *dmsB-2*, SO_4357–58). Both loci are still present in ΔOMC, the parental strain of suppressor mutant ΔOMC^S. Hence, *dmsAB-1* and *dmsAB-2* were deleted in ΔOMC^S and the effect of these deletions on the Fe(III) citrate reduction rate of this strain was sought. The deletions did not lead to a change of the ΔOMC^S phenotype with respect to Fe(III) citrate reduction (data not shown). Hence, an involvement of these proteins in the described iron reduction phenotype was excluded.

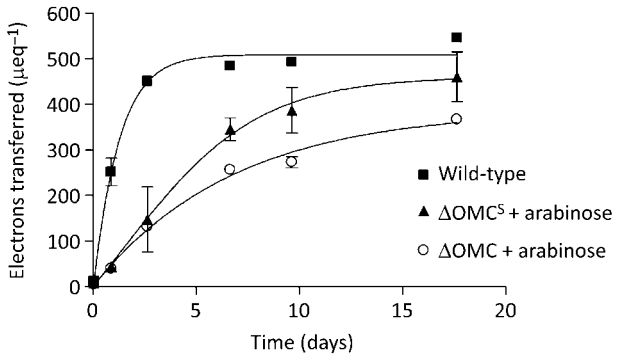

Fig. 5. Humic acid reduction. Electrons transferred to PPHA by different *S. oneidensis* strains. Values are given in electron equivalents measured with Fe(III) citrate in an electron shuttling assay. Symbols show means of duplicate measurements; error bars, SD. Solid lines represent curve-fits done with GraphPad Prism 4. The specific PPHA reduction rate, μ, in h^{-1} was calculated for each biological replicate, and the mean ± SD values are: wild-type, 0.534 ± 0.045; ΔOMC^S + arabinose, 0.451 ± 0.104; ΔOMC^S, not determinable; ΔOMC + arabinose, not determinable.

The type II secretion system transfers outer-membrane cytochromes to the outer surface of the cell in *S. oneidensis*. Consequently, this export machinery is essential for metal reduction (DiChristina *et al.*, 2002; Shi *et al.*, 2008). If other proteins could functionally replace the outer-membrane cytochromes in ΔOMC^S, one would expect a possible involvement of type II secretion in protein translocation. The genes for the type II secretion systems are clustered in the *gsp* locus. Deletion of *gspD*, a key gene within the cluster, is sufficient to disable the function of the secretion system (Shi *et al.*, 2008). As expected, *gspD*

deletion led to a complete loss of ferric reductase activity using the wild-type as parental strain (Fig. 6). In contrast to this, the ΔOMC^{S}Δ*gspD* (JG444) strain was not affected in Fe(III) citrate reduction, since the maximal reduction rates of ΔOMC^S and ΔOMC^{S}Δ*gspD* were almost identical. Only a slightly longer lag phase of the ΔOMC^{S}Δ*gspD* strain was detectable, which might be due to a slightly lower initial cell number (Fig. 6).

Confirmation of outer-membrane integrity in ΔOMC^S

A higher permeability of the outer membrane could cause the observed phenotype of ΔOMC^S, since it is known that periplasmic cytochromes can catalyse ferric iron reduction as well (Pitts *et al.*, 2003; Qian *et al.*, 2011b; Schuetz *et al.*, 2009). Still, outer-membrane cytochromes are usually necessary, since electron acceptors such as Fe(III) citrate or birnessite cannot pass the outer membrane. Therefore, three tests were performed to exclude the possibility that the general stability or permeability of the outer membrane might be the reason for the observed phenotype of the ΔOMC^S-mutant. First ethidium bromide uptake rates were determined by measuring the increase in fluorescence over time. Ethidium bromide is a large, hydrophobic dye (about 12 Å wide) with a delocalized positive charge that makes it unlikely to diffuse through narrow porin channels (7 × 11 Å in *E. coli* OmpF; Cowan *et al.*, 1992). It can therefore be used to measure the permeability of the outer membrane (Murata *et al.*, 2007). The detected ethidium bromide uptake kinetics of wild-type, ΔOMC and ΔOMC^S were almost identical (Fig. S2). As a positive control, cells were treated with polymyxin B, which destabilizes the outer membrane (Vaara, 1992). The ethidium bromide uptake rate increased approximately twofold (Fig. S2a) but was again identical in the three tested strains. A similar experiment was performed with Fe(III) citrate as a second test to exclude the possibility that a more specific Fe(III) citrate transporter could cause the observed reduction phenotype. The amount of Fe(III) citrate diffusion into the cell was determined after 30 min incubation. The total cellular iron content after washing the cells was nearly identical for all strains but increased when polymyxin B was added (Fig. S2b).

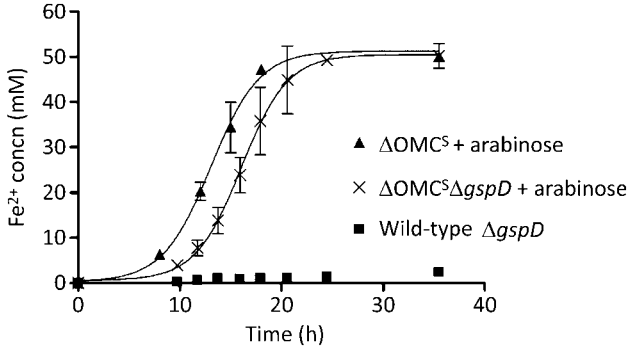

Fig. 6. Fe(III) citrate reduction with *gspD* mutants. Fe(III) citrate reduction by *S. oneidensis* Δ*gspD* mutant, ΔOMC^S and ΔOMC^{S}Δ*gspD* mutant strains growing on minimal medium with 50 mM lactate and 50 mM Fe(III) citrate. Arabinose was added to all experiments at a concentration of 1 mM. Means of triplicate measurements are shown; error bars, SD. Solid lines represent curve-fits done with GraphPad Prism 4. The specific iron reduction rate, μ, in h^{-1} was calculated for each biological replicate, and the mean ± SD values are: ΔOMC^{S}Δ*gspD* + arabinose, 0.445 ± 0.082; ΔOMC^S + arabinose, 0.451 ± 0.104. The reduction rate for wild-type Δ*gspD* was not determinable because a curve-fit was not possible due to minimal reduction within the time frame of the experiment.

As a third test, the antibiotic susceptibility of the different strains was compared using kanamycin A as an aminoglycoside, colistin as a polymixine, and chloramphenicol, which forms its own group of small molecules with an aromatic ring. As Fig. S3 indicates, the inhibitory zones around the test plates containing the antibiotic drugs were either very similar for wild-type, ΔOMC and ΔOMC^S or smaller for ΔOMC^S compared with the other two strains. Therefore, the results of the ethidium bromide and Fe(III) citrate uptake tests were verified, and it seems unlikely that an altered outer-membrane permeability caused the observed phenotype of ΔOMC^S.

Identification of point mutations as a genetic basis of ΔOMC suppression

The genetic source of the ΔOMC^S mutant phenotype was addressed using Solexa sequencing of the genome and mapping to the published sequence of *S. oneidensis* MR-1 (accession no. NC_004347). The genome was nearly completely covered (>99.9 % coverage). Analysis of the assembled Solexa reads revealed 85 point mutations but no larger insertions or rearrangements of genes (Table S2). Two of the point mutations raised our interest, since they were localized in *mtrA* and *mtrB*, respectively. In both cases, a nucleotide base exchange of cytosine to adenosine occurred. These exchanges resulted in the replacement of an asparagine by a lysine in MtrA and MtrB, respectively (MtrA, Asn 290 Lys; MtrB, Asn 219 Lys; numbers refer to the amino acid sequence of MtrA and MtrB, and the corresponding chromosomal positions are 1 858 407 and 1 857 606, respectively). The secondary structure of the mutated MtrB protein was predicted using PRED-TMBB (Bagos *et al.*, 2004). The mutation was found to be located in the middle of a hydrophilic stretch.

Both proteins are crucial for dissimilatory metal reduction as well as reduction of extracellular electron shuttles. Furthermore, arabinose induction was necessary for extracellular respiration in ΔOMC^S. Therefore, it was our aim to assess whether these point mutations in *mtrA* and *mtrB* caused the observed ΔOMC^S phenotype. Hence, both genes were cloned in their wild-type and suppressor mutant form (designated *mtrA*^{S} and *mtrB*^{S}) in a pBAD202 expression

Table 2. Plasmids used in this study

Plasmid	Relevant genotype	Source or reference
pBAD202	Expression vector, Km^r, arabinose-inducible promoter	Invitrogen
pMQ150	Deletion vector, cen/arsh, *ura3*, Km^r, *sacB*	Shanks *et al.* (2006); accession no. EU546823
$pmtrA^S$	*mtrA* with nucleic base exchange C869A in pBAD202	This study
$pmtrB^S$	*mtrB* with nucleic base exchange C656A in pBAD202	This study
pmtrAmtrB	*mtrA* and *mtrB* in pBAD202	This study
$pmtrA^SmtrB^S$	*mtrA* C869A and *mtrB* C656A in pBAD202	This study
$pmtrAmtrB^S$	*mtrA* and *mtrB* C656A in pBAD202	This study

vector, resulting in plasmids pmtrAmtrB and $pmtrA^SmtrB^S$ (Table 2). These plasmids were transferred into the parental strain ΔOMC and the resulting strains were tested for their ability to reduce Fe(III) citrate (Fig. 7). Expression of the wild-type allele (strain JG450) did not lead to an alteration of the ΔOMC phenotype, but expression of the allele carrying the point mutations (strain JG449) resulted in a phenotype highly similar to ΔOMC^S (Fig. 7). Since these data demonstrated that the point mutations in $mtrA^S$ and $mtrB^S$ were essential for suppression of the ΔOMC^S mutation, it was concluded that the other observed point mutations might be interesting but were of minor importance for this study.

A further question arising this study was whether a single mutated gene is sufficient for ferric iron reduction without outer-membrane cytochromes. Therefore, $mtrA^S$ and $mtrB^S$ were cloned into separate vectors, resulting in $pmtrA^S$ and $pmtrB^S$ (strains JG462 and 463). Expression of both proteins could be shown by SDS-PAGE (Fig. S4). Only $mtrB^S$ expression (strain JG463) resulted in iron reduction, although at a lower level compared with ΔOMC^S or the ΔOMC strain carrying $pmtrA^SmtrB^S$ (Fig. 7). Hence, both variants, $MtrA^S$ and $MtrB^S$, have to be present to enable rapid reduction of Fe(III) citrate.

Complementation of Δ*mtrA* and Δ*mtrB* mutants using $mtrA^S$ and $mtrB^S$

MtrA and MtrB form a complex in the outer membrane of *S. oneidensis* cells (Hartshorne *et al.*, 2009). Furthermore, MtrA is necessary for the periplasmic stability of MtrB (Schicklberger *et al.*, 2011). Since this interaction seems to be highly specific, it was asked whether the observed point mutations led to variants of the corresponding proteins that were only able to operate in the presence of the other variant. In other words, can $MtrB^S$ only operate in an $MtrA^S$ strain or is an interaction with wild-type MtrA still possible? Consequently, $mtrA^S$ and $mtrB^S$ were expressed in *S. oneidensis* Δ*mtrA* and Δ*mtrB* strains, respectively. As Fig. S5 indicates, both genes can also complement the corresponding deletion mutants in a wild-type background. Hence, the point mutations do not seem to be localized to positions that disable interaction with the wild-type partner proteins.

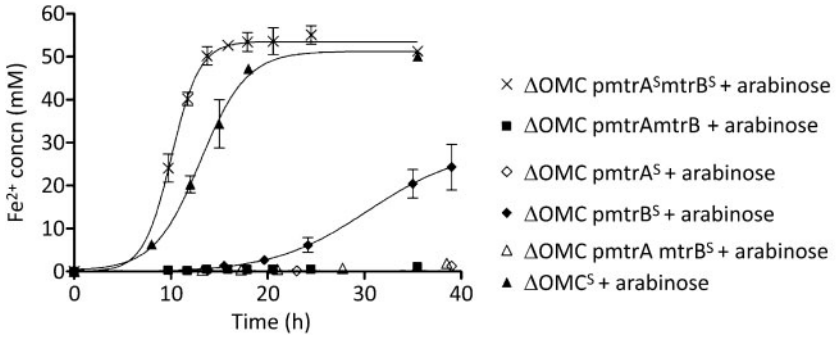

Fig. 7. ΔOMC complementation with pmtr plasmids. Fe(III) citrate reduction by *S. oneidensis* ΔOMC mutant strains, complemented with different plasmids and growing on minimal medium with 50 mM lactate and 50 mM Fe(III) citrate. Arabinose was added to all experiments at a concentration of 1 mM. Means of triplicate measurements are shown; error bars, SD. Solid lines represent curve-fits done with GraphPad Prism 4. The specific iron reduction rate, μ, in h^{-1} was calculated for each biological replicate, and the mean ± SD values are: ΔOMC $pmtrA^SmtrB^S$, 0.602 ± 0.169; ΔOMC pmtrAmtrB, not determinable; ΔOMC $pmtrA^S$, not determinable; ΔOMC $pmtrB^S$, 0.218 ± 0.062; ΔOMC $pmtrAmtrB^S$, not determinable; ΔOMC^S, 0.451 ± 0.104. Some reduction rates were not determinable because curve-fits were not possible due to minimal reduction within the time frame of the experiment.

MtrAB clusters in microbial genomes

Respiration of extracellular electron acceptors without outer-membrane cytochromes may be a strategy that is used by other micro-organisms as well. Hence, it was asked whether clusters consisting of genes encoding a periplasmic decahaem cytochrome and β-barrel protein can be found in the database that are not accompanied by a gene encoding an outer-membrane decahaem cytochrome like MtrF or MtrC directly upstream or downstream. Twenty-five gene clusters with similarities to *mtrAB* from *S. oneidensis* were detected using the integrated microbial genomes tool (Table 3). Six of these clusters belong to purple bacteria. One of these purple bacteria strains, *Rhodopseudomonas palustris* TIE-1, has been shown to be dependent on this gene cluster when ferrous iron is added as electron donor for photolithotrophic growth (Jiao & Newman, 2007). The *pioAB* genes are similar to *mtrAB*, and they are accompanied by a gene encoding a periplasmic high-potential iron protein that has been suggested to enable periplasmic electron transfer between PioAB and, tentatively, the photosystem in the inner membrane of the organism (Bird *et al.*, 2011). The similarities between *pioABC* of *R. palustris* TIE-1 and all other *mtrAB*-like clusters in *Rhodopseudomonas* and *Rhodomicrobium* strains suggest a similar function in these purple bacteria as well. Interestingly, *Gallionella capsiferriformans* (also known as *Gallionella ferruginea*, subsp. *capsiferriformans*) and *Siderooxydans lithotrophicus* also contain *mtrAB*-like gene cassettes. Both organisms are known to use the neutrophilic oxidation of ferrous iron with oxygen as energy source (Emerson *et al.*, 2010). Furthermore, similar clusters *were* detected in other organisms, including nitrifiers, sulfate reducers and magnetotactic bacteria. Of note, a number of *Geobacter* strains contain similar clusters as well. Some of these clusters contain a β-barrel protein that has either low or almost no similarity to MtrB from *S. oneidensis*. So far it is not possible to ascribe a function to these gene clusters, but it seems possible that they enable some kind of extracellular respiration, be it electron uptake as in the case of PioABC or electron disposal.

DISCUSSION

Mesophilic dissimilatory metal reducers like *S. oneidensis* MR-1 have developed an extended respiratory chain to the cell surface. This respiratory chain is mainly composed of *c*-type cytochromes (Shi *et al.*, 2007). In previous work we have shown that expression of the cytoplasmic membrane *c*-type cytochrome CymA is sufficient to transform *E. coli* into a dissimilatory iron reducer. Still, this respiratory process is possible only when soluble, outer membrane-permeable iron chelates such as Fe(III)-NTA are used (Gescher *et al.*, 2008). Environmentally relevant electron acceptors such as ferrihydrite, haematite or birnessite are poorly soluble or effectively insoluble at neutral pH (Thamdrup, 2000). Hence, their reduction depends on electron transfer through the periplasm and outer membrane. As already mentioned in the Introduction, even some chelated ferric iron sources like Fe(III) citrate are apparently not membrane-permeable (Dobbin *et al.*, 1996; Gescher *et al.*, 2008; Pitts *et al.*, 2003). Large, polymeric Fe(III) citrate complexes that are observed under certain conditions might explain this effect (Spiro *et al.*, 1967). It is therefore not surprising that the catabolic reduction of Fe(III) citrate in *S. oneidensis* depends on the catalytic activity of outer-membrane cytochromes. Interestingly, Qian and co-workers proposed an OMC-independent iron chelate uptake mechanism catalysed by SO_2907 and subsequent periplasmic ferric iron reduction (Qian *et al.*, 2011a). This would certainly challenge the assumption that Fe(III) citrate can be used as a model substance to study extracellular respiration. Nevertheless, the ΔOMC strain is unable to reduce Fe(III) citrate at detectable rates (Bücking *et al.*, 2010). Furthermore, several different laboratories have demonstrated that mutants in *mtrC*, *mtrB* or *mtrA* are unable to grow with Fe(III) citrate as electron acceptor (Beliaev & Saffarini, 1998; Beliaev *et al.*, 2001; Borloo *et al.*, 2007; Hartshorne *et al.*, 2009; Myers & Myers, 2002b). MtrA, MtrB and MtrC build the electron conduit to the cell surface, and MtrC is probably the most influential terminal reductase for extracellular respiration in *S. oneidensis* (Belchik *et al.*, 2011; Beliaev *et al.*, 2001; Coursolle *et al.*, 2010; Jiao *et al.*, 2011; Marshall *et al.*, 2006; Reardon *et al.*, 2010). All this seems to be in disagreement with the experiments conducted by Qian and co-workers. Those authors found that a deletion mutant in a gene encoding a putative TonB-dependent receptor protein (SO_2907) was affected in ferric iron reduction. Still, they observed that the corresponding protein is an efficient Fe(III)-NTA binding protein. Hence, the observed growth phenotype might also be caused by the lack of an efficient iron acquisition protein in the outer membrane of an SO_2907 deletion mutant. Furthermore, and unfortunately, they did not show complementation of the mutant using SO_2907. Hence, it is not absolutely clear whether a polar effect of the mutation also accounts at least partly for the observed growth disadvantage.

As pointed out above, MtrC is believed to be the main terminal metal and flavin reductase. The phenotype of a Δ*mtrC* mutant can only be rescued if MtrC itself or the similar cytochrome MtrF is used for complementation (Bücking *et al.*, 2010; Myers & Myers, 2001). Hence, it was a great surprise to see that a quintuple mutant in all outer-membrane cytochrome-encoding genes (ΔOMC) was able to regain its ability to grow as a dissimilatory metal reducer after a lag phase of several weeks. The new strain, ΔOMC^{S}, reduced Fe(III) citrate nearly as fast as the wild-type in growth experiments. Interestingly, the suppressor mutant reduced extracellular electron acceptors with varying activities when compared with the wild-type in cell suspension experiments. Fe(III) citrate and AQDS were reduced with rates ranging from >50 to 99 % compared with the recorded wild-type reduction rates. In contrast,

riboflavin, PPHA and birnessite were reduced at only 20–35 % compared with the wild-type. The different redox potentials of these compounds are unlikely to be the reason for the observed differences. Fe(III) citrate has a potential of +372 mV (Straub *et al.*, 2001), while AQDS, with −184 mV, is more than half a volt below this value (Fultz & Durst, 1982). Birnessite has a redox potential of +612 mV (Robie *et al.*, 1995) and is therefore an even better electron acceptor than Fe(III) citrate. The redox potential of riboflavin is, at −210 mV (Stare, 1935), very similar to the potential of AQDS. For naturally occurring humic acids, no defined redox potentials, but rather ranges of standard reduction potentials from +150 to 300 mV (at pH 7), have been determined (Aeschbacher *et al.*, 2011), since they form a supermolecular association of very diverse organic molecules. Still, since redox potentials are most likely not the reason for the observed kinetic data, we hypothesize that substrate specificity causes the observed differences. This substrate specificity would be determined by the terminal reductase of ΔOMC^S. Our experiments suggest that $MtrA^S$ is the novel terminal reductase in this strain. Evidence for this hypothesis comes from the results of the mutant experiments conducted. These experiments revealed (i) that no outer-membrane cytochrome is involved in extracellular reduction of ΔOMC^S, (ii) that the DMSO reductase is not required as a terminal reductase of Fe(III) citrate, (iii) that export of other potential reductases via the type II secretion system is not required, and finally (iv) that $MtrA^S$ and $MtrB^S$ are both essential for the extracellular reduction of ΔOMC^S. MtrB is a typical outer-membrane β-barrel protein, that most probably has a structural but not an enzymic function (Hartshorne *et al.*, 2009; Myers & Myers, 2002a). In contrast, MtrA is a *c*-type cytochrome that has been shown to have ferric iron reductase activity (Pitts *et al.*, 2003). Hence, we hypothesize that the point mutations enable $MtrA^S$ to contact electron acceptors at the cell surface, or that the pore of $MtrB^S$ is – when compared with wild-type MtrB – altered in a way that allows extracellular electron acceptors to reach the inside of the pore and hence contact $MtrA^S$. This second hypothesis would be in line with the results of the cell suspension experiments. Larger substances are reduced more slowly than smaller electron acceptors, independently of their redox potential. Riboflavin, birnessite and PPHA might just be too large to reach the inside of the pore in the same way as Fe(III) citrate or AQDS. Still, we cannot definitely discount the possibility that other surface-localized proteins could interact with $MtrA^S$ and/or $MtrB^S$ and hence could also be involved in the observed phenotype.

Unfortunately, it is so far not possible to show how the point mutations that exchange asparagine residues for lysine residues would enable this hypothesized modified structure of the $MtrAB^S$ complex. The crystal structure of the two important proteins, MtrA and MtrB, is not known so far. The mutation in MtrB was predicted to localize to a hydrophilic stretch outside the β-barrel, and one could speculate that this stretch might be important for the interaction between MtrA and MtrB. The structure of MtrA was modelled recently by Firer-Sherwood *et al.* (2011) based on small-angle X-ray scattering. They proposed an elongated form of MtrA, which fits well with a partial insertion into the barrel of MtrB to form a complex. The point mutation in $MtrA^S$ is near the C-terminal region and could be embedded into MtrB.

The ability of the suppressor mutant to reduce extracellular electron acceptors without outer-membrane cytochromes raises the question of whether this suppressor mutant resembles an evolutionary intermediate. The correct localization of outer-membrane cytochromes is a complex process. Lipid anchors have to be added to periplasmic cytochromes. These modified cytochromes have to be recognized by the type II secretion machinery. This machinery is a multiprotein complex itself, but furthermore the interaction with target proteins is highly specific and still not fully understood (Francetić & Pugsley, 2005; Sandkvist, 2001). Last but not least, these outer-membrane cytochromes have to be connected to modules such as MtrAB that thereafter can deliver electrons that originate from the cytoplasmic membrane. Due to this complexity it seems likely that the addition of outer-membrane cytochromes to existing outer-membrane conduits might be a typical example of upstream evolution. We were able to show that extracellular metal respiration is possible without outer-membrane cytochromes, although the environment might have finally selected for organisms with higher reduction rates realized by outer-membrane cytochromes. Interestingly, bioinformatic investigations revealed similarities to known ferrous iron oxidizers such as the chemolithotrophs *Gallionella capsiferriformans* and *Siderooxydans lithotrophicus*, and the photolithotrophic purple bacterium *R. palustris* TIE-1. For *R. palustris* TIE-1 and *Siderooxydans lithotrophicus* ES-1 it is known that genes similar to MtrAB are necessary for ferrous iron oxidation (Jiao & Newman, 2007; Liu *et al.*, 2012). For the latter, it has been shown that MtoA from *Siderooxydans lithotrophicus* can functionally replace MtrA in *Shewanella* (Liu *et al.*, 2012). One could envisage a succession from a module necessary for ferrous iron oxidation in one species to a module that is necessary for the reverse reaction in another species. It should be noted that there might be further metabolic processes that depend on MtrAB-like complexes, since similar gene clusters were also detected in other organisms. Future research will reveal their role in the individual organisms.

Finally, it should be mentioned that the studied suppressor mutant nicely displays the plasticity of *S. oneidensis*. In a previous publication a similar case was observed but not followed. Myers & Myers (2002b) could show in their experiments that a Δ*mtrC* mutant was capable of reducing Fe(III) citrate after a 3-day lag phase. The cells that were growing after 72 h might also have been suppressor mutants. What we can learn is that the results of mutant studies have to be treated carefully, at least in *S. oneidensis*.

Table 3. Gene clusters with similarities to *mtrAB* from *S. oneidensis*

(a), (b), (c): These genomes contain two or more MtrAB homologues.

Genome	MtrA homologue	Expected E value	Number of amino acid residues	MtrB homologue	Expected E value	Number of amino acid residues	Gene upstream of MtrA homologue	Size of intergenic region before MtrA	Function of gene upstream of MtrA
Desulfobacterium autotrophicum HRM2	HRM2_13960	4E-44	323	HRM2_13950	−*	583	HRM2_13970	466 bp	Dicarboxylate transporter protein†
Desulfuromonas acetoxidans DSM 684	Dace_1556	9E-43	354	Dace_1557	−*	805	Not sequenced	Not sequenced	Unknown
Gallionella capsiferriformans ES-2	Galf_2004	2E-63	343	Galf_2003	1E-23	792	Galf_2005	69 bp	Cytochrome *c* class I (very small, 112 aa)‡
Geobacter bemidjiensis Bem, DSM 16622	Gbem_3118	4E-38	334	Gbem_3117	−*	718	Gbem_3119	1 bp	ABC transporter-related protein
Geobacter sp. FRC-32	Geob_2912	3E-39	331	Geob_2911	−*	701	Geob_2913	1 bp	ABC transporter-related
Geobacter sp. M18 (a)	GM18_0932	2E-08	192	GM18_0933	−*	660	GM18_0931	60 bp	NHL repeat-containing protein
Geobacter sp. M18 (b)	GM18_1019	3E-07	192	GM18_1020	−*	653	GM18_1018	18 bp	NHL repeat-containing protein
Geobacter sp. M18 (c)	GM18_3089	1E-42	340	GM18_3088	−*	762	GM18_3090	1 bp	ABC transporter-like protein
Geobacter sp. M21 (a)	GM21_0397	7E-66	299	GM21_0398	3E-16	807	GM21_0396	367 bp	Transcriptional regulator
Geobacter sp. M21 (b)	GM21_1144	3E-44	334	GM21_1145	−*	716	GM21_1143	1 bp	ABC transporter-related
Geobacter uraniireducens Rf4 (a)	Gura_2291	7E-46	335	Gura_2290	−*	712	Gura_2292	1 bp	ABC transporter-related
Geobacter uraniireducens Rf4 (b)	Gura_3626	1E-61	299	Gura_3627	1E-17	835	Gura_3625	486 bp	Transcriptional regulator
Magnetospirillum magneticum AMB-1	amb3017	6E-63	318	amb3018	2E-21	731	amb3016	3 bp	Hypothetical
Nitrosococcus halophilus Nc4 (a)	Nhal_1192	7E-59	325	Nhal_1191	2E-21	827	Nhal_1193‡	38 bp	NUDIX hydrolase
Nitrosococcus halophilus Nc4 (b)	Nhal_1655	1E-76	312	Nhal_1654	1E-75	755	Nhal_1656	75 bp	Peptidoglycan-binding LysM
Nitrosococcus oceani AFC27	NOC27_2654	7E-45	168	NOC27_3054	1E-07	461	NOC27_2862	51 bp	Hypothetical
Nitrosococcus oceani ATCC 19707	Noc_2748	−*	315	Noc_2747	2E-27	827	Noc_2749	44 bp	NUDIX hydrolase†
Rhodomicrobium vannielii ATCC 17100	Rvan_3213	2E-48	476	Rvan_3214	2E-06	844	Rvan_3212	468 bp	Exonuclease RecJ
R. palustris BisA53	RPE_0831	9E-49	632	RPE_0832	2E-13	793	RPE_0830	754 bp	Alpha/beta hydrolase
R. palustris BisB18	RPC_2960	1E-45	577	RPC_2959	1E-14	830	RPC_2961†	545 bp	Putative flavoprotein involved in K^+ transport
R. palustris CGA009	RPA0746	5E-48	534	RPA0745	1E-08	810	*cysA*	775 bp	*cysA*, putative sulfate ABC transporter

Table 3. cont.

Genome	MtrA homologue	Expected E value	Number of amino acid residues	MtrB homologue	Expected E value	Number of amino acid residues	Gene upstream of MtrA homologue	Size of intergenic region before MtrA	Function of gene upstream of MtrA
R. palustris DX-1	Rpdx1_0796	7E-48	548	Rpdx1_0795	2E-11	810	Rpdx1_0797	548 bp	Sulfate ABC transporter ATPase subunit
R. palustris TIE-1	Rpal_0817	4E-48	540	Rpal_0816	2E-08	810	Rpal_0818	742 bp	Sulfate ABC transporter, ATPase subunit
Siderooxydans lithotrophicus ES-1	Slit_2497	4E-57	355	Slit_2496	2E-20	810	Slit_2498	45 bp	Cytochrome *c* class I (very small, 117 aa)*
Sutterella wadsworthensis							HMPREF9464_01980	1E-49	
								293	
HMPREF9464_01981	–*						HMPREF9464_01979	506 bp	Hypothetical†
		637							
S. oneidensis MR-1	SO_1777		333	SO_1776		697	*mtrC*	69 bp	Decahaem *c*-type cytochrome (671 aa)

*These genes are predicted to encode β-barrel proteins (http://biophysics.biol.uoa.gr/PRED-TMBB/), but the E value of a BLAST search against MtrB is above 1E-5.
†These proteins are not predicted to be lipoproteins by LipoP (http://www.cbs.dtu.dk/services/LipoP/).
‡These genes are encoded in the opposite direction to *mtrA*.

The shorter the duration of an experiment, the more one can exclude the possibility that the observed phenotype might not be due to the inserted genetic modification but to a suppressor mutation. Therefore, Fe(III) citrate seems to be a good model substance to study extracellular electron transport pathways, since it allows fast growth and reduction rates when compared with mineral phase electron acceptors such as ferrihydrite or haematite.

In conclusion, this study characterizes for the first time MtrA and MtrB as a final reductase necessary for extracellular respiration. Only two point mutations were necessary to gain this activity. It seems possible that this form of dissimilatory metal reduction resembles a preliminary form which might have been the intermediate state between lithotrophic ferrous iron oxidization and heterotrophic ferric iron respiration.

REFERENCES

Aeschbacher, M., Vergari, D., Schwarzenbach, R. P. & Sander, M. (2011). Electrochemical analysis of proton and electron transfer equilibria of the reducible moieties in humic acids. *Environ Sci Technol* **45**, 8385–8394.

Bagos, P. G., Liakopoulos, T. D., Spyropoulos, I. C. & Hamodrakas, S. J. (2004). A Hidden Markov Model method, capable of predicting and discriminating β-barrel outer membrane proteins. *BMC Bioinformatics* **5**, 29.

Bayer, M., Walter, K. & Simon, H. (1996). Purification and partial characterisation of a reversible artificial mediator accepting NADH oxidoreductase from *Clostridium thermoaceticum*. *Eur J Biochem* **239**, 686–691.

Belchik, S. M., Kennedy, D. W., Dohnalkova, A. C., Wang, Y., Sevinc, P. C., Wu, H., Lin, Y., Lu, H. P., Fredrickson, J. K. & Shi, L. (2011). Extracellular reduction of hexavalent chromium by cytochromes MtrC and OmcA of *Shewanella oneidensis* MR-1. *Appl Environ Microbiol* **77**, 4035–4041.

Beliaev, A. S. & Saffarini, D. A. (1998). *Shewanella putrefaciens mtrB* encodes an outer membrane protein required for Fe(III) and Mn(IV) reduction. *J Bacteriol* **180**, 6292–6297.

Beliaev, A. S., Saffarini, D. A., McLaughlin, J. L. & Hunnicutt, D. (2001). MtrC, an outer membrane decahaem *c* cytochrome required for metal reduction in *Shewanella putrefaciens* MR-1. *Mol Microbiol* **39**, 722–730.

Bird, L. J., Bonnefoy, V. & Newman, D. K. (2011). Bioenergetic challenges of microbial iron metabolisms. *Trends Microbiol* **19**, 330–340.

Boogerd, F. C. & de Vrind, J. P. (1987). Manganese oxidation by *Leptothrix discophora*. *J Bacteriol* **169**, 489–494.

Borloo, J., Vergauwen, B., De Smet, L., Brigé, A., Motte, B., Devreese, B. & Van Beeumen, J. (2007). A kinetic approach to the dependence of dissimilatory metal reduction by *Shewanella oneidensis* MR-1 on the outer membrane cytochromes *c* OmcA and OmcB. *FEBS J* **274**, 3728–3738.

Bradford, M. M. (1976). A rapid and sensitive method for the quantitation of microgram quantities of protein utilizing the principle of protein-dye binding. *Anal Biochem* **72**, 248–254.

Bücking, C., Popp, F., Kerzenmacher, S. & Gescher, J. (2010). Involvement and specificity of *Shewanella oneidensis* outer membrane cytochromes in the reduction of soluble and solid-phase terminal electron acceptors. *FEMS Microbiol Lett* **306**, 144–151.

Burdige, D. J. & Nealson, K. H. (1985). Microbial manganese reduction by enrichment cultures from coastal marine sediments. *Appl Environ Microbiol* **50**, 491–497.

Coursolle, D. & Gralnick, J. A. (2010). Modularity of the Mtr respiratory pathway of *Shewanella oneidensis* strain MR-1. *Mol Microbiol* **77**, 995–1008.

Coursolle, D., Baron, D. B., Bond, D. R. & Gralnick, J. A. (2010). The Mtr respiratory pathway is essential for reducing flavins and electrodes in *Shewanella oneidensis*. *J Bacteriol* **192**, 467–474.

Cowan, S. W., Schirmer, T., Rummel, G., Steiert, M., Ghosh, R., Pauptit, R. A., Jansonius, J. N. & Rosenbusch, J. P. (1992). Crystal structures explain functional properties of two *E. coli* porins. *Nature* **358**, 727–733.

DiChristina, T. J., Moore, C. M. & Haller, C. A. (2002). Dissimilatory Fe(III) and Mn(IV) reduction by *Shewanella putrefaciens* requires *ferE*, a homolog of the *pulE* (*gspE*) type II protein secretion gene. *J Bacteriol* **184**, 142–151.

Dobbin, P. S., Warren, L. H., Cook, N. J., McEwan, A. G., Powell, A. K. & Richardson, D. J. (1996). Dissimilatory iron(III) reduction by *Rhodobacter capsulatus*. *Microbiology* **142**, 765–774.

El-Naggar, M. Y., Wanger, G., Leung, K. M., Yuzvinsky, T. D., Southam, G., Yang, J., Lau, W. M., Nealson, K. H. & Gorby, Y. A. (2010). Electrical transport along bacterial nanowires from *Shewanella oneidensis* MR-1. *Proc Natl Acad Sci U S A* **107**, 18127–18131.

Emerson, D., Fleming, E. J. & McBeth, J. M. (2010). Iron-oxidizing bacteria: an environmental and genomic perspective. *Annu Rev Microbiol* **64**, 561–583.

Firer-Sherwood, M. A., Ando, N., Drennan, C. L. & Elliott, S. J. (2011). Solution-based structural analysis of the decaheme cytochrome, MtrA, by small-angle X-ray scattering and analytical ultracentrifugation. *J Phys Chem B* **115**, 11208–11214.

Francetić, O. & Pugsley, A. P. (2005). Towards the identification of type II secretion signals in a nonacylated variant of pullulanase from *Klebsiella oxytoca*. *J Bacteriol* **187**, 7045–7055.

Fultz, M. L. & Durst, R. A. (1982). Mediator compounds for the electrochemical study of biological redox systems: a compilation. *Anal Chim Acta* **140**, 1–18.

Gescher, J. S., Cordova, C. D. & Spormann, A. M. (2008). Dissimilatory iron reduction in *Escherichia coli*: identification of CymA of *Shewanella oneidensis* and NapC of *E. coli* as ferric reductases. *Mol Microbiol* **68**, 706–719.

Gibson, D. G., Young, L., Chuang, R. Y., Venter, J. C., Hutchison, C. A., III & Smith, H. O. (2009). Enzymatic assembly of DNA molecules up to several hundred kilobases. *Nat Methods* **6**, 343–345.

Gorby, Y. A., Yanina, S., McLean, J. S., Rosso, K. M., Moyles, D., Dohnalkova, A., Beveridge, T. J., Chang, I. S., Kim, B. H. & other authors (2006). Electrically conductive bacterial nanowires produced by *Shewanella oneidensis* strain MR-1 and other microorganisms. *Proc Natl Acad Sci U S A* **103**, 11358–11363.

Gralnick, J. A., Vali, H., Lies, D. P. & Newman, D. K. (2006). Extracellular respiration of dimethyl sulfoxide by *Shewanella oneidensis* strain MR-1. *Proc Natl Acad Sci U S A* **103**, 4669–4674.

Hartshorne, R. S., Reardon, C. L., Ross, D., Nuester, J., Clarke, T. A., Gates, A. J., Mills, P. C., Fredrickson, J. K., Zachara, J. M. & other authors (2009). Characterization of an electron conduit between bacteria and the extracellular environment. *Proc Natl Acad Sci U S A* **106**, 22169–22174.

Jiang, J. & Kappler, A. (2008). Kinetics of microbial and chemical reduction of humic substances: implications for electron shuttling. *Environ Sci Technol* **42**, 3563–3569.

Jiao, Y. & Newman, D. K. (2007). The *pio* operon is essential for phototrophic Fe(II) oxidation in *Rhodopseudomonas palustris* TIE-1. *J Bacteriol* **189**, 1765–1773.

Jiao, Y., Qian, F., Li, Y., Wang, G., Saltikov, C. W. & Gralnick, J. A. (2011). Deciphering the electron transport pathway for graphene oxide reduction by *Shewanella oneidensis* MR-1. *J Bacteriol* **193**, 3662–3665.

Laemmli, U. K. (1970). Cleavage of structural proteins during the assembly of the head of bacteriophage T4. *Nature* **227**, 680–685.

Li, H. & Durbin, R. (2009). Fast and accurate short read alignment with Burrows–Wheeler transform. *Bioinformatics* **25**, 1754–1760.

Li, H., Handsaker, B., Wysoker, A., Fennell, T., Ruan, J., Homer, N., Marth, G., Abecasis, G., Durbin, R. & 1000 Genome Project Data Processing Subgroup (2009). The sequence alignment/map format and SAMtools. *Bioinformatics* **25**, 2078–2079.

Liu, J., Wang, Z., Belchik, S. M., Edwards, M. J., Liu, C., Kennedy, D. W., Merkley, E. D., Lipton, M. S., Butt, J. N. & other authors (2012). Identification and characterization of MtoA: a decaheme *c*-type cytochrome of the neutrophilic Fe(II)-oxidizing bacterium *Sideroxydans lithotrophicus* ES-1. *Front Microbiol* **3**, 37.

Lovley, D. R., Coates, J. D., Blunt-Harris, E. L., Phillips, E. J. P. & Woodward, J. C. (1996). Humic substances as electron acceptors for microbial respiration. *Nature* **382**, 445–448.

Lower, B. H., Yongsunthon, R., Shi, L., Wildling, L., Gruber, H. J., Wigginton, N. S., Reardon, C. L., Pinchuk, G. E., Droubay, T. C. & other authors (2009). Antibody recognition force microscopy shows that outer membrane cytochromes OmcA and MtrC are expressed on the exterior surface of *Shewanella oneidensis* MR-1. *Appl Environ Microbiol* **75**, 2931–2935.

Lutz, R. & Bujard, H. (1997). Independent and tight regulation of transcriptional units in *Escherichia coli* via the LacR/O, the TetR/O and AraC/I1-I2 regulatory elements. *Nucleic Acids Res* **25**, 1203–1210.

Marshall, M. J., Beliaev, A. S., Dohnalkova, A. C., Kennedy, D. W., Shi, L., Wang, Z., Boyanov, M. I., Lai, B., Kemner, K. M. & other authors (2006). *c*-Type cytochrome-dependent formation of U(IV) nanoparticles by *Shewanella oneidensis*. *PLoS Biol* **4**, e268.

Marsili, E., Baron, D. B., Shikhare, I. D., Coursolle, D., Gralnick, J. A. & Bond, D. R. (2008). *Shewanella* secretes flavins that mediate extracellular electron transfer. *Proc Natl Acad Sci U S A* **105**, 3968–3973.

Meyer, T. E., Tsapin, A. I., Vandenberghe, I., de Smet, L., Frishman, D., Nealson, K. H., Cusanovich, M. A. & van Beeumen, J. J. (2004). Identification of 42 possible cytochrome *c* genes in the *Shewanella oneidensis* genome and characterization of six soluble cytochromes. *OMICS* **8**, 57–77.

Milne, I., Bayer, M., Cardle, L., Shaw, P., Stephen, G., Wright, F. & Marshall, D. (2010). Tablet—next generation sequence assembly visualization. *Bioinformatics* **26**, 401–402.

Murata, T., Tseng, W., Guina, T., Miller, S. I. & Nikaido, H. (2007). PhoPQ-mediated regulation produces a more robust permeability barrier in the outer membrane of *Salmonella enterica* serovar Typhimurium. *J Bacteriol* **189**, 7213–7222.

Myers, J. M. & Myers, C. R. (2001). Role for outer membrane cytochromes OmcA and OmcB of *Shewanella putrefaciens* MR-1 in reduction of manganese dioxide. *Appl Environ Microbiol* **67**, 260–269.

Myers, C. R. & Myers, J. M. (2002a). MtrB is required for proper incorporation of the cytochromes OmcA and OmcB into the outer membrane of *Shewanella putrefaciens* MR-1. *Appl Environ Microbiol* **68**, 5585–5594.

Myers, J. M. & Myers, C. R. (2002b). Genetic complementation of an outer membrane cytochrome *omcB* mutant of *Shewanella putrefaciens*

MR-1 requires *omcB* plus downstream DNA. *Appl Environ Microbiol* **68**, 2781–2793.

Myers, J. M. & Myers, C. R. (2003). Overlapping role of the outer membrane cytochromes of *Shewanella oneidensis* MR-1 in the reduction of manganese(IV) oxide. *Lett Appl Microbiol* **37**, 21–25.

Myers, C. R. & Nealson, K. H. (1988a). Bacterial manganese reduction and growth with manganese oxide as the sole electron acceptor. *Science* **240**, 1319–1321.

Myers, C. R. & Nealson, K. H. (1988b). Microbial reduction of manganese oxides: interactions with iron and sulfur. *Geochim Cosmochim Acta* **52**, 2727–2732.

Pitts, K. E., Dobbin, P. S., Reyes-Ramirez, F., Thomson, A. J., Richardson, D. J. & Seward, H. E. (2003). Characterization of the *Shewanella oneidensis* MR-1 decaheme cytochrome MtrA: expression in *Escherichia coli* confers the ability to reduce soluble Fe(III) chelates. *J Biol Chem* **278**, 27758–27765.

Qian, Y., Shi, L. & Tien, M. (2011a). SO2907, a putative TonB-dependent receptor, is involved in dissimilatory iron reduction by *Shewanella oneidensis* strain MR-1. *J Biol Chem* **286**, 33973–33980.

Qian, Y., Paquete, C. M., Louro, R. O., Ross, D. E., Labelle, E., Bond, D. R. & Tien, M. (2011b). Mapping the iron binding site(s) on the small tetraheme cytochrome of *Shewanella oneidensis* MR-1. *Biochemistry* **50**, 6217–6224.

Reardon, C. L., Dohnalkova, A. C., Nachimuthu, P., Kennedy, D. W., Saffarini, D. A., Arey, B. W., Shi, L., Wang, Z., Moore, D. & other authors (2010). Role of outer-membrane cytochromes MtrC and OmcA in the biomineralization of ferrihydrite by *Shewanella oneidensis* MR-1. *Geobiology* **8**, 56–68.

Reguera, G., McCarthy, K. D., Mehta, T., Nicoll, J. S., Tuominen, M. T. & Lovley, D. R. (2005). Extracellular electron transfer via microbial nanowires. *Nature* **435**, 1098–1101.

Richter, K., Bücking, C., Schicklberger, M. & Gescher, J. (2010). A simple and fast method to analyze the orientation of *c*-type cytochromes in the outer membrane of Gram-negative bacteria. *J Microbiol Methods* **82**, 184–186.

Robie, R. A., Huebner, J. S. & Hemingway, B. S. (1995). Heat-capacities and thermodynamic properties of braunite (Mn_7SiO_{12}) and rhodonite ($MnSiO_3$). *Am Mineral* **80**, 560–575.

Roden, E. E., Kappler, A., Bauer, I., Jiang, J., Paul, A., Stoesser, R., Konishi, H. & Xu, H. (2010). Extracellular electron transfer through microbial reduction of solid-phase humic substances. *Nat Geosci* **3**, 417–421.

Romine, M. F., Carlson, T. S., Norbeck, A. D., McCue, L. A. & Lipton, M. S. (2008). Identification of mobile elements and pseudogenes in the *Shewanella oneidensis* MR-1 genome. *Appl Environ Microbiol* **74**, 3257–3265.

Ross, D. E., Brantley, S. L. & Tien, M. (2009). Kinetic characterization of OmcA and MtrC, terminal reductases involved in respiratory electron transfer for dissimilatory iron reduction in *Shewanella oneidensis* MR-1. *Appl Environ Microbiol* **75**, 5218–5226.

Saltikov, C. W. & Newman, D. K. (2003). Genetic identification of a respiratory arsenate reductase. *Proc Natl Acad Sci U S A* **100**, 10983–10988.

Sandkvist, M. (2001). Biology of type II secretion. *Mol Microbiol* **40**, 271–283.

Schicklberger, M., Bücking, C., Schuetz, B., Heide, H. & Gescher, J. (2011). Involvement of the *Shewanella oneidensis* decaheme cytochrome MtrA in the periplasmic stability of the β-barrel protein MtrB. *Appl Environ Microbiol* **77**, 1520–1523.

Schuetz, B., Schicklberger, M., Kuermann, J., Spormann, A. M. & Gescher, J. (2009). Periplasmic electron transfer via the *c*-type cytochromes MtrA and FccA of *Shewanella oneidensis* MR-1. *Appl Environ Microbiol* **75**, 7789–7796.

Shanks, R. M., Caiazza, N. C., Hinsa, S. M., Toutain, C. M. & O'Toole, G. A. (2006). *Saccharomyces cerevisiae*-based molecular tool kit for manipulation of genes from Gram-negative bacteria. *Appl Environ Microbiol* **72**, 5027–5036.

Shi, L., Chen, B., Wang, Z., Elias, D. A., Mayer, M. U., Gorby, Y. A., Ni, S., Lower, B. H., Kennedy, D. W. & other authors (2006). Isolation of a high-affinity functional protein complex between OmcA and MtrC: two outer membrane decaheme *c*-type cytochromes of *Shewanella oneidensis* MR-1. *J Bacteriol* **188**, 4705–4714.

Shi, L., Squier, T. C., Zachara, J. M. & Fredrickson, J. K. (2007). Respiration of metal (hydr)oxides by *Shewanella* and *Geobacter*: a key role for multihaem *c*-type cytochromes. *Mol Microbiol* **65**, 12–20.

Shi, L., Deng, S., Marshall, M. J., Wang, Z., Kennedy, D. W., Dohnalkova, A. C., Mottaz, H. M., Hill, E. A., Gorby, Y. A. & other authors (2008). Direct involvement of type II secretion system in extracellular translocation of *Shewanella oneidensis* outer membrane cytochromes MtrC and OmcA. *J Bacteriol* **190**, 5512–5516.

Shyu, J. B., Lies, D. P. & Newman, D. K. (2002). Protective role of *tolC* in efflux of the electron shuttle anthraquinone-2,6-disulfonate. *J Bacteriol* **184**, 1806–1810.

Spiro, T. G., Pape, L. & Saltman, P. (1967). Hydrolytic polymerization of ferric citrate. I. Chemistry of polymer. *J Am Chem Soc* **89**, 5555–5559.

Stare, F. J. (1935). A potentiometric study of hepatoflavin. *J Biol Chem* **112**, 223–229.

Stevenson, F. (1994). *Humus Chemistry: Genesis, Composition, Reactions*. New York: Wiley.

Stookey, L. L. (1970). Ferrozine—a new spectrophotometric reagent for iron. *Anal Chem* **42**, 779–781.

Straub, K. L., Benz, M. & Schink, B. (2001). Iron metabolism in anoxic environments at near neutral pH. *FEMS Microbiol Ecol* **34**, 181–186.

Thamdrup, B. (2000). Bacterial manganese and iron reduction in aquatic sediments. *Adv Microb Ecol* **16**, 41–84.

Thomas, P. E., Ryan, D. & Levin, W. (1976). An improved staining procedure for the detection of the peroxidase activity of cytochrome P-450 on sodium dodecyl sulfate polyacrylamide gels. *Anal Biochem* **75**, 168–176.

Vaara, M. (1992). Agents that increase the permeability of the outer membrane. *Microbiol Rev* **56**, 395–411.

Venkateswaran, K., Moser, D. P., Dollhopf, M. E., Lies, D. P., Saffarini, D. A., MacGregor, B. J., Ringelberg, D. B., White, D. C., Nishijima, M. & other authors (1999). Polyphasic taxonomy of the genus *Shewanella* and description of *Shewanella oneidensis* sp. nov. *Int J Syst Bacteriol* **49**, 705–724.

von Canstein, H., Ogawa, J., Shimizu, S. & Lloyd, J. R. (2008). Secretion of flavins by *Shewanella* species and their role in extracellular electron transfer. *Appl Environ Microbiol* **74**, 615–623.

Xiong, Y., Shi, L., Chen, B., Mayer, M. U., Lower, B. H., Londer, Y., Bose, S., Hochella, M. F., Fredrickson, J. K. & Squier, T. C. (2006). High-affinity binding and direct electron transfer to solid metals by the *Shewanella oneidensis* MR-1 outer membrane *c*-type cytochrome OmcA. *J Am Chem Soc* **128**, 13978–13979.

Zhang, H., Tang, X., Munske, G. R., Zakharova, N., Yang, L., Zheng, C., Wolff, M. A., Tolic, N., Anderson, G. A. & other authors (2008). In vivo identification of the outer membrane protein OmcA–MtrC interaction network in *Shewanella oneidensis* MR-1 cells using novel hydrophobic chemical cross-linkers. *J Proteome Res* **7**, 1712–1720.

Edited by: R. J. Maier